

# Fair DARTS: Eliminating Unfair Advantages in Differentiable Architecture Search

Xiangxiang Chu<sup>1</sup> Tianbao Zhou<sup>2†\*</sup> Bo Zhang<sup>1†</sup> Jixiang Li<sup>1</sup>

<sup>1</sup>Xiaomi AI Lab, <sup>2</sup>Minzu University of China

<sup>1</sup>{chuxiangxiang, zhangbo11, lijixiang}@xiaomi.com, <sup>2</sup>tianbaochou@163.com

## Abstract

*Differential Architecture Search (DARTS) is now a widely disseminated weight-sharing neural architecture search method. However, there are two fundamental weaknesses remain untackled. First, we observe that the well-known aggregation of skip connections during optimization is caused by an **unfair advantage** in an **exclusive competition**. Second, there is a non-negligible incongruence when discretizing continuous architectural weights to a one-hot representation. Because of these two reasons, DARTS delivers a biased solution that might not even be suboptimal. In this paper, we present a novel approach to curing both frailties. Specifically, as unfair advantages in a pure exclusive competition easily induce a monopoly, we relax the choice of operations to be collaborative, where we let each operation have an equal opportunity to develop its strength. We thus call our method Fair DARTS. Moreover, we propose a **zero-one** loss to directly reduce the discretization gap. Experiments are performed on two mainstream search spaces, in which we achieve new state-of-the-art networks on ImageNet. Our code is available here<sup>1</sup>.*

## 1. Introduction

In the wake of the DARTS’s open-sourcing [18], a diverse number of its variants emerge in the *neural architecture search* community. Some of them extend its use in higher-level architecture search spaces with performance awareness in mind [4, 29], some learn a stochastic distribution instead of architectural parameters [29, 30, 33, 7, 8], and others offer remedies on discovering its lack of robustness [21, 5, 16, 13, 32].

In spite of these endeavors, Why is there an obvious increase in the number of skip connections [5]? (see Figure 1) What makes a one-hot pruned subnetwork perform poorly

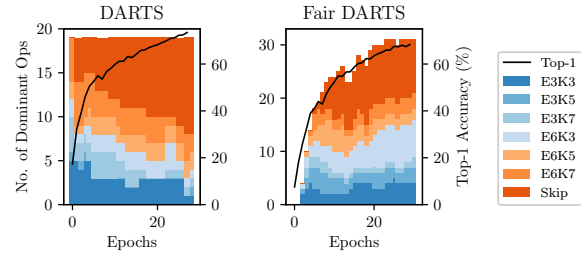


Figure 1. The number of dominant operations (in all 19 layers) of DARTS and Fair DARTS searching on ImageNet (in search space  $S_2$ ). In DARTS, skip connections incrementally suppress others. In Fair DARTS, all operations develop independently.

while its supernet<sup>2</sup> converges quite well [32]?

In this paper, we mainly discuss in-depth about these failure modes of DARTS. In particular, the ResNet [10]-like nature of skip connections interferes with the training of the supernet, which continues boosting their priors against others. Meanwhile, such dominant skip connections in the continuous supernet can’t directly be discretized, otherwise causing a dramatic performance drop. To avoid these two major issues, we propose a novel approach named Fair DARTS, in which we discuss current robustifying methods [5, 16, 32] on DARTS with a unified fairness perspective. To summarize, we have the following contributions.

**Firstly**, we discover two major causes that hinder better performance of DARTS. The first is what we later define as an **unfair advantage** that drives skip connections into a monopoly state in an **exclusive competition**. These two indispensable factors work together to induce a performance collapse. The second is the inherent inequality lying in discretization that can produce a dramatic discrepancy.

**Secondly**, we propose the first *collaborative competition* approach to resolve these two issues. By offering each operation an independent architectural weight, the unfair advantage no longer prevails. We again minimize the discretization gap with a novel auxiliary loss, called *zero-one loss*, to

<sup>1</sup> <https://github.com/xiaomi-automl/fairdarts>

<sup>1</sup>\*:Work done as an intern. <sup>†</sup>: Equal contribution.

<sup>2</sup>Despite minor ambiguities and for simplicity, we hereby refer to the overall network that encompasses all child models as a ‘supernet’.

steer architectural weights towards their extremities, that is, either completely enabled or disabled. The inequality thus decreases to its minimum.

**Thirdly**, we provide a unified perspective to view current DARTS cures for skip connections. The majority of these works either make use of dropout [26] on skip connections [5, 32], or play with the later termed *boundary epoch* by different early-stopping strategies [16, 32]. We instead, fundamentally eliminate unfair competition with no other restrictions at all. Moreover, based on our observations, we derive a hypothesis that adding Gaussian noise can also disrupt the unfairness, which is later proved to be effective.

**Lastly**, we conduct thorough experiments in two widely used search spaces in both proxy and proxyless ways. Results show that our method can escape from performance collapse. We also achieve state-of-the-art networks on CIFAR-10 and ImageNet.

## 2. Related Works

Due to the limit of the DARTS search space, ProxylessNAS [4] and FBNet [29] apply DARTS in much larger search spaces based on MobileNetV2 [24]. ProxylessNAS also differs from DARTS in its supernet training process, where only two paths are activated, based on the assumption that one path is the best amongst all should be better than any single one. From a fairness point of view, as only two paths enhance their ability (get parameters updated) while others remain unchanged, it implicitly creates a bias. FB-Net [29], SNAS [30] and GDAS [8] utilize the differentiable Gumbel Softmax [20, 12] to mimic one-hot encoding. However, the one-hot nature implies an exclusive competition, which risks being exploited by unfair advantages.

SETN [7] combines one-shot methodology [3, 1] with DARTS [18] by learning a stochastic evaluator to sample models of low validation loss. Once trained, this evaluator is used to select 1k one-shot models to decide the final best architecture. As the supernet is optimized with uniform sampling, unfairness is reduced to some extent. But its evaluator utilizes *softmax* for categorical distribution, which suffers the same issue as DARTS does.

The aggregation of skip connections in DARTS has been noticed by many [5, 16, 2, 32]. As a quick remedy, PDARTS [5] utilizes dropout as a workaround to restrict the number of skip connections. DARTS+ [16] puts a hard limit of two skip-connections per cell. However, it is better not to enforce such strong human priors. Besides, the discretization gap is acknowledged by DARTS [18] but later mostly neglected by its followers. RobustDARTS [32] blames this gap for poor generalization and proposes an early stopping method to avoid solutions of a sharp minimum.

Superficially, the most relevant work to ours is RobustDARTS [32]. Under several simplified search spaces, they state that the found solutions generalize poorly when they

coincide with high validation loss curvature, where the supernet with an excessive number of skip connections happens to be such a solution. Our method is quite distinct from it, because we study the underlying mechanism that leads to bad solutions instead of their characteristics.

## 3. The Darkness of DARTS

In this section, we aim to excavate the dark side of DARTS that possibly impedes the searching performance. We first prepare a minimum background.

### 3.1. Preliminary of Differentiable Architecture Search

For the case of convolutional neural networks, DARTS [18] searches for a *normal cell* and a *reduction cell* to build up the final architecture. A cell is represented as a directed acyclic graph (DAG) of  $N$  nodes in sequential order. Each node stands for a feature map. The edge  $e_{i,j}$  from node  $i$  to  $j$  operates on the input feature  $x_i$  and its output is denoted as  $o_{i,j}(x_i)$ . The intermediate node  $j$  gathers all inputs from the incoming edges,

$$x_j = \sum_{i < j} o_{i,j}(x_i). \quad (1)$$

Let  $\mathcal{O} = \{o_{i,j}^1, o_{i,j}^2, \dots, o_{i,j}^M\}$  be the set of  $M$  candidate operations on edge  $e_{i,j}$ . DARTS relaxes this categorical choice to a softmax over all operations in  $\mathcal{O}$  to form a mixed output:

$$\bar{o}_{i,j}(x) = \sum_{o \in \mathcal{O}} \frac{\exp(\alpha_{o_{i,j}})}{\sum_{o' \in \mathcal{O}} \exp(\alpha_{o'_{i,j}})} o(x), \quad (2)$$

where each operation  $o_{i,j}$  is associated with a continuous coefficient  $\alpha_{o_{i,j}}$ . Regarding edge  $e_{i,j}$ , this softmax is utilized to approximate one-hot encoding  $\beta_{i,j} = (\beta_{o_{i,j}^1}, \beta_{o_{i,j}^2}, \dots, \beta_{o_{i,j}^M})$ . Formally, let  $\alpha_{o_{i,j}}$  denote the architectural weights vector  $(\alpha_{o_{i,j}^1}, \alpha_{o_{i,j}^2}, \dots, \alpha_{o_{i,j}^M})$ . DARTS thus assumes the following as a valid approximation,

$$\text{softmax}(\alpha_{o_{i,j}}) \approx \beta_{i,j}. \quad (3)$$

The architecture search problem is reduced to learning  $\alpha^*$  and network weights  $w^*$  that minimize the validation loss  $\mathcal{L}_{val}(w^*, \alpha^*)$ . DARTS resolves this problem with a bi-level optimization,

$$\begin{aligned} & \min_{\alpha} \mathcal{L}_{val}(w^*(\alpha), \alpha) \\ & \text{s.t. } w^*(\alpha) = \text{argmin}_w \mathcal{L}_{train}(w, \alpha). \end{aligned} \quad (4)$$

We also adopt two common search spaces, the DARTS [18] search space ( $S_1$ ) and the ProxylessNAS [4] search space ( $S_2$ ) with minor modifications. The details are given in Section B.

In  $S_2$ , the output of the  $l$ -th layer is a softmax-weighted summation of  $N$  choices. Formally, it can be written as

$$x_l = \sum_{k=1}^N \frac{\exp(\alpha_{l-1,l}^k)}{\sum_{j=1}^N \exp(\alpha_{l-1,l}^j)} o_{l-1,l}^k(x_{l-1}). \quad (5)$$

### 3.2. Performance Downfall Caused by Intractable Skip Connections

DARTS suffers significant performance decay when *skip connections* become dominant [5, 16]. It was described as a competition-and-cooperation issue in the bi-level optimization [16]. Still, the reason behind this behavior is not clear, we hereby need a different perspective.

First, to confirm this issue, we run DARTS  $k = 4$  times with the same random seed. Following DARTS, we select 8 top-performing operations per cell (2 each for 4 intermediate nodes). Here we say one operation is *dominating* if it has top-2  $\text{softmax}(\alpha)$  among all incoming edges' candidates of a certain node. The results are shown in Figure 2. In the beginning, all operations are given the same opportunity. As the over-parameterized network gradually converges, there is an evident aggregation of skip connections after 20 epochs (5 out of 8 in an extreme case), detrimentally worsening the performance of the resulting architecture.

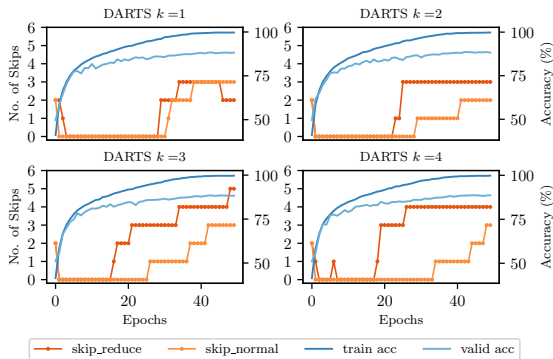


Figure 2. The number of dominating skip connections continues to grow when searching with DARTS (run 4 times) on CIFAR-10 (in  $S_1$ ). Train and validation accuracies are also drawn to show the level of convergence.

When we utilize DARTS directly on ImageNet in  $S_2$ , which is a single branch architecture, the same phenomenon rigorously reappears. The number of dominant skip-connections (highest  $\text{softmax}(\alpha)$  among all operations in that layer) steadily increases and reaches 11 out of 19 layers in the end, which is shown on the left of Figure 1.

But why is this happening? The underlying reasons are rarely discussed in depth. A brief and superficial analysis regarding information flow is given in [5]. However, we claim that the reason for excessive skip connections is from **exclusive competition** among various operations. In

Equation 2 and Equation 5, the skip connection is softmax-weighted and added to the output. The softmax operation inherently provides an exclusive competition since increasing one is at the cost of suppressing others. Moreover, this weighted sum resembles a basic residual module in ResNet [10], which states that it benefits the training of deep neural networks. Therefore, its architectural weight increases much faster than its competitors. As a result, the skip connection becomes gradually dominant during optimization. Note an extra advantage and an exclusive competition are two indispensable factors to cause the performance collapse. Note that the skip connection works cooperatively with convolutions in [10]. Whereas, in DARTS, the final architecture is obtained by picking only the top-performing ones among all competitive operations, which breaks this cooperation.

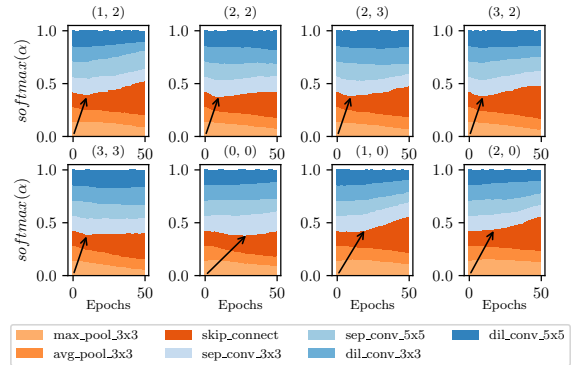


Figure 3. The softmax evolution where skip connections gradually become dominant when running DARTS on CIFAR-10 (in  $S_1$ ). Last two subplots of edge (1,0) and (2,0) are from the normal cell, the rest are from reduction cell. Black arrows point to boundary epochs where skip connections start to demonstrate its strength.

We further study this effect from the experiments on CIFAR-10 by recording the competition progress in Figure 3. The derived model has 8 skip connections in total<sup>3</sup>. ResNet [10] discovers that *skip connections begin to demonstrate power after a few epochs compared with that without skip connections*, interestingly, a similar phenomenon is also observed in our experiments. In our method, we term this tipping point a *boundary epoch*. The boundary epochs may vary from edge to edge, but are generally at the early stage. From Figure 3, we observe that skip connections colored in red-orange progressively obtain higher architectural weights after some certain boundary epochs. Meantime, other operations are suppressed and steadily decline. We consider this benefit from residual module as an unfair advantage by Definition 1.

**Definition 1. Unfair Advantage.** Suppose that choosing one operation amongst others is a competition. This com-

<sup>3</sup>corresponding to the experiment ( $k = 3$ ) in Figure 2.

petition is deemed **exclusive** when only one operation can be selected. An operation in an exclusive competition is said to have an **unfair advantage** if this advantage contributes more to competition than to the performance of a resulted network.

From this discussion, we can draw the following insight,

**Insight 1: The root cause of excessive skip connections is the inherent unfair competition.** The skip connection has an unfair advantage by forming a residual module which is convenient for the training of supernet, but not equally beneficial for the performance of the outcome network.

Suppose the above analysis is solid and we take steps to allow collaboration, we can expect an outcome that after the first few epochs, some other operations in addition to skip connections can also have progressively higher architectural weights, despite the increasing speed being bit slower. We will check it later in Section 5.3.

Moreover, we discover another interesting fact while searching on ImageNet in  $S_2$ ,

**Observation:** The supernet with many dominant skip connections has outstanding performance but its derived child network behaves poorly. a) The supernet at the last epoch obtains 73% top-1 accuracy with 11 skip connections on the ImageNet validation dataset, which is shown on the left of Figure 1. b) The child network generated from the *argmax* operation obtained only 66.39% when trained from scratch, shown in Table 1.

This observation appears so counter-intuitive at first glance. However, it is directly caused by the discrepancy of discretization as will be discussed later.

### 3.3. Non-negligible Discrepancy of Discretization

DARTS reports that it may suffer from discrepancies when discretizing continuous encodings [18]. It also suggests annealing softmax could alleviate the issue. It is thus important to investigate how much does such discrepancy harm the search performance. Two fundamental problems are worthy of deep analysis. One is that under what conditions does the continuous relaxation (Equation 2) hold, the other is to know when it fails and how to avoid it.

The answer to the first question seems trivial because the  $k$ -th output of softmax must be dominantly larger than the others to approximate  $m_{l,k} = 1$  with good accuracy. Let's check to what extent does DARTS approximate this ideal condition.

We run DARTS on CIFAR-10 and display  $\text{softmax}(\alpha)$  of the last iteration in Figure 4. The largest value is about 0.3 while the smallest one is above 0.1<sup>4</sup>. On one hand, it is not a good approximation to meet Equation 3, i.e., this leads to a **non-negligible gap** between the derived model and its

<sup>4</sup>We run DARTS 4 times and it holds every time.

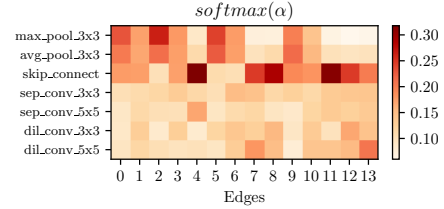


Figure 4. Heatmap of softmax values in the last searching epoch when running DARTS on CIFAR-10 (in search space  $S_1$ ).

Models	Top-1 Acc (%)
Continuous supernet (at the end of searching)	73.48
Discretized subnetwork (trained from scratch)	66.39 ( $\downarrow$ 7.89)

Table 1. Performance discrepancy of DARTS's discretization. A supernet with many dominant skip connections performs well while the discretized model behave poorly.

supernet, as observed in Section 3.2. In the worst cases, the gap becomes so large that it turns into pure noise for choice selection.

On the other hand, the range is too narrow to differentiate between ‘good’ and ‘bad’ operations. For instance in Figure 4, the top-2 highest values are very close on the 1st, 3rd, 6th, and 9th edge. It’s hard to say that an edge weighted by 0.26 is better than another by 0.24.

Furthermore, we perform a parallel experiment in  $S_2$  on ImageNet which is given in Figure 5. There are 7 deeper layers whose softmax values of skip connection are above 0.8. In the shallow layers, they are more or less evenly distributed. From Table 1, the whole supernet obtains 73.48% top-1 accuracy within 30 epochs. By contrast, the derived model trained 300 epochs from scratch only reaches 66.39%. In this experiment, many highly weighted *parameter-free* operations (e.g., skip connections) win against those with learnable parameters. This serves as one failure case for  $S_2$  as we select one operation out of  $N$  competitive candidates. Hence, we learn the second insight:

**Insight 2: Relaxing from discrete categorical choices to continuous ones should make a good approximation.**

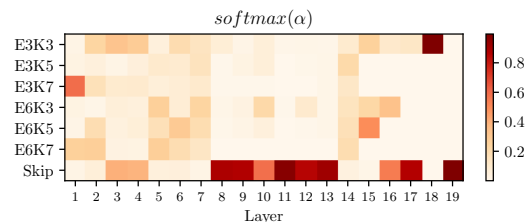


Figure 5. Heatmap of softmax values in the last searching epoch when running DARTS in  $S_2$ . Many skip connections aggregate.

## 4. The Fair DARTS

### 4.1. Stepping out the Pitfalls of Skip Connections by Cooperation

Based on **Insight 1**, we propose a cooperative mechanism to eliminate the existing unfair advantage. Not only should we exploit skip connection for smoother information flow, but we also have to provide equal opportunities for other operations. In a word, they need to avoid being trapped by unfair advantage from skip connections. On this regard, we apply a *sigmoid activation* for each  $\alpha_{i,j}$ , so that each operation can be switched on or off independently without being suppressed. Formally, we replace Equation 2 with,

$$\bar{o}_{i,j}(x) = \sum_{o \in \mathcal{O}} \sigma(\alpha_{o_{i,j}}) o(x). \quad (6)$$

It's trivial to show that even if  $\sigma(\alpha_{skip})$  saturates at 1, other operations still can be optimized cooperatively. Promising operations continue to grow their weights to reduce  $\mathcal{L}_{val}$ . With  $\sigma(\alpha)$  defined, the gap problem remains. We still need to find out how to drive it towards extremities (0 and 1) to alleviate the discussed discrepancy of discretization.

### 4.2. Minimizing the gap of Discretization

Inspired by **Insight 2**, we explicitly coerce an extra loss called *zero-one loss* to push the sigmoid value of architectural weights towards 0 or 1. Let  $L_{0-1} = f(z)$  denote this loss component, where  $z = \sigma(\alpha)$ . To achieve our goal, the loss design must meet three basic criteria, a) It needs to have a global maximum at  $z = 0.5$  (a fair starting point) and a global minimum at 0 and 1. b) The gradient magnitude  $\frac{df}{dz}|_{z=0.5}$  has to be adequately small to allow architectural weights to fluctuate, but large enough to attract  $z$  towards 0 or 1 when they are a bit far from 0.5. c) It should be differentiable for back propagation.

By the first requirement, we move  $\sigma(\alpha)$  away from 0.5 towards 0 or 1 to minimize the discretization gap. The second one enacts explicit necessary constraints. Particularly, small gradients around the peak avoids stepping easily into two ends. Larger gradients around 0 and 1 instead help to quickly capture  $z$  nearby.

Quite straightforward, we come up with a loss function to meet the above requirements, formally as,

$$L_{0-1} = -\frac{1}{N} \sum_i^N (\sigma(\alpha_i) - 0.5)^2 \quad (7)$$

In order to control its strength, we weight this loss by a coefficient  $w_{0-1}$ , thus the total loss for  $\alpha$  is formulated as,

$$L_{total} = \mathcal{L}_{val}(w^*(\alpha), \alpha) + w_{0-1} L_{0-1}. \quad (8)$$

Like DARTS [18], the architectural weight can be optimized through back propagation. From Equation 8, the search objective is to find an architecture of high accuracy with a good approximation from continuous to discrete.

Moreover, the second requirement is indispensable, otherwise the gradient-based approach may step into local minimum too early. Here we design another loss as a negative example. Let  $L'_{0-1}$  be the following,

$$L'_{0-1} = -\frac{1}{N} \sum_i^N |(\sigma(\alpha_i) - 0.5)|. \quad (9)$$

It's trivial to see that  $\frac{d|z-0.5|}{dz}|_{z>0.5} = 1$  and  $\frac{d|z-0.5|}{dz}|_{z<0.5} = -1$ . Once  $z$  stays away from 0.5, it may receive the same gradient (1 or -1) in the later iterations, thus rapidly pushing the architectural weights towards two ends. This phenomenon is illustrated in Figure 6.

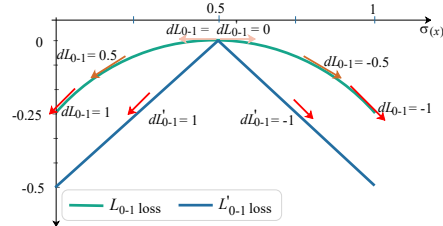


Figure 6. Illustration about the auxiliary loss design:  $L_{0-1}$  (proposed) and  $L'_{0-1}$  (control).

By combining Equation 4, 6 and 8, our method which we call Fair DARTS, can be now formally written as

$$\begin{aligned} & \min_{\alpha} \mathcal{L}_{val}(w^*(\alpha), \alpha) + w_{0-1} L_{0-1} \\ \text{s.t. } & w^*(\alpha) = \operatorname{argmin}_w \mathcal{L}_{train}(w, \alpha). \\ & \bar{o}_{i,j}(x) = \sum_{o \in \mathcal{O}} \sigma(\alpha_{o_{i,j}}) o(x). \end{aligned} \quad (10)$$

## 5. Experiments and Results

### 5.1. Searching Architectures for CIFAR-10

At the search stage, we use similar hyperparameters and tricks as [18]. We apply the *first-order* optimization and it takes 10 GPU hours. All experiments are done on a Tesla V100. We select our target models with  $\sigma_{threshold} = 0.85$ <sup>5</sup>. We use the same data processing and training trick as [18, 5].

To verify the robustness of our approach, we repetitively search 7 times on several seeds and report the number of skip connections in Figure 8 (shown 4). An average error rate of 2.59% is obtained. Especially, FairDARTS-a, the smallest one, obtains 2.54% error rate on CIFAR-10 with

<sup>5</sup>We choose operations whose  $\sigma$  are above  $\sigma_{threshold}$ . The maximum number of edges for a node is limited to 2.

reduced parameters and multiply-adds. We draw the cells of FairDARTS-a in Figure 7, others are included in Table 8.

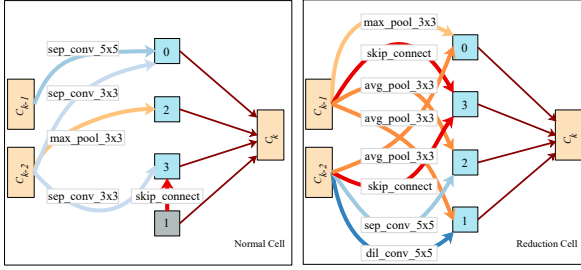


Figure 7. FairDARTS-a cells searched on CIFAR-10 in  $S_1$ .

The normal cell of FairDARTS-a is rather simple and only 3 nodes are activated, which is previously rarely seen. In the reduction cell, more edges are activated to compensate for the information loss due to down-sampling. As reduction cells are of small proportion, FairDARTS-a thus retains to be lightweight.

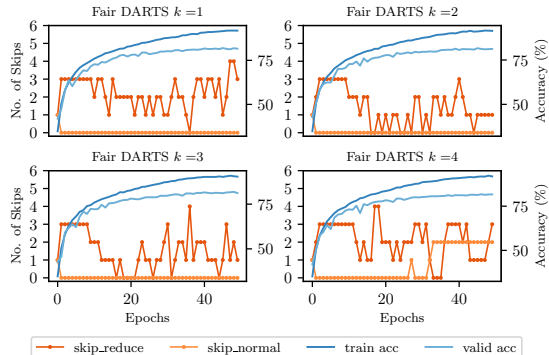


Figure 8. The number of dominating skip connections when searching with Fair DARTS on CIFAR-10. Here we select top-2 operations as dominants as in DARTS (our proposed way selects dominants according to  $\sigma_{threshold}$ ), our method can still escape from too many skip connections.

## 5.2. Transferring to ImageNet

As a common practice, we transfer two searched cells (FairDARTS-a and b<sup>6</sup>) to the ImageNet. We keep the same configuration and use the identical training tricks as DARTS [18]. Compared with SNAS [30] and DARTS, FairDARTS-A only uses 3.6M number of parameters and 417M multiply-adds to obtain 73.7% top-1 accuracy on ImageNet validation dataset. FairDARTS-B also achieves state-of-the-art 75.1% in  $S_1$  with a smaller number of parameters than comparable counterparts.

<sup>6</sup>Its architecture is given in Figure 17.

Models	Params (M)	$\times +$ (M)	Test Error (%)	Type
NASNet-A [35]	3.3	608 <sup>†</sup>	2.65	RL
ENAS [22]	4.6	626 <sup>†</sup>	2.89	RL
MdeNAS[33]	3.6	599 <sup>†</sup>	2.55	MDL
DARTS [18]	3.3	528 <sup>†</sup>	2.86	GD
SNAS [30]	2.9	422 <sup>†</sup>	2.98	GD
GDAS [8]	3.37	519 <sup>†</sup>	2.93	GD
P-DARTS [5]	3.4	532 <sup>†</sup>	2.5	GD
PC-DARTS [31]	3.6	558 <sup>†</sup>	2.57	GD
RDARTS [32]	-	-	2.95	GD
FairDARTS-a	<b>2.8</b>	<b>371</b>	2.54	GD
FairDARTS <sup>‡</sup>	$3.27 \pm 0.48$	$458 \pm 61$	$2.59 \pm 0.14$	GD

Table 2. Comparison of architectures on CIFAR-10. <sup>†</sup>: MultAdds computed using the genotypes provided by the authors. <sup>‡</sup>: Averaged on models from 7 runs of Fair DARTS.

Models	$\times +$ (M)	Params (M)	Top-1 (%)	Top-5 (%)	Cost*
MobileNetV2 [24]	585	6.9	74.7	-	-
NASNet-A [35]	564	5.3	74.0	91.6	2000
AmoebaNet-A[23]	555	5.1	74.5	92.0	3150
MnasNet-92 [27]	388	3.9	74.79	92.1	-
MdeNAS[33]	-	6.1	74.5	92.1	2
DARTS [18]	574	4.7	73.3	91.3	4
PNAS [17]	588	5.1	74.2	91.9	255
FBNet-C [29]	375	5.5	74.9	-	9
Proxyless GPU [4] <sup>‡</sup>	465 <sup>*</sup>	7.1	75.1	-	8.3
FairNAS-C [?] <sup>‡</sup>	321	4.4	74.7	92.1	10
SNAS [30]	522	4.3	72.7	90.8	1.5
GDAS [8]	581	5.3	74.0	91.5	0.21
P-DARTS [5] <sup>††</sup>	577	5.1	74.9*	92.3*	0.3
PC-DARTS [31] <sup>†</sup>	586	5.3	74.9	92.2	3.8
FairDARTS-A <sup>†</sup>	417	3.6	73.7	91.7	0.4
FairDARTS-B <sup>†</sup>	541	4.8	75.1	92.5	0.4
FairDARTS-C <sup>‡</sup>	380	4.2	75.1	92.4	3
FairDARTS-D <sup>‡</sup>	440	4.3	<b>75.6</b>	<b>92.6</b>	3

Table 3. Comparison of architectures on ImageNet. \*: Based on its published code. <sup>†</sup>: Searched on CIFAR-10. <sup>††</sup>: Searched on CIFAR-100. <sup>‡</sup>: Searched on ImageNet. \*: in GPU days.

## 5.3. Searching Proxylessly on ImageNet

In ProxylessNAS [4], there are 19 searchable layers and each layer contains 7 choices, consisting of  $7^{19}$  possible models. In our approach, every choice can be activated independently, thus,  $S_2$  contains  $2^{133} = 128^{19}$  possible models. To our knowledge, this is a most gigantic search space ever proposed, being  $18^{19}$  times that of [4].

For the search phase, we search 30 epochs with a batch size of 1024, which takes about 3 GPU days. The final architectural weight matrix (after sigmoid activation) in Figure 10 is used to derive target models. Note that skip connections are preferred from layer 2 to 12. Under this cooperative setting, other inverted bottleneck blocks can work together with skip connections, where the former learn the residual information and the latter facilitate the training [15]. In contrast, under the competitive setting of DARTS,

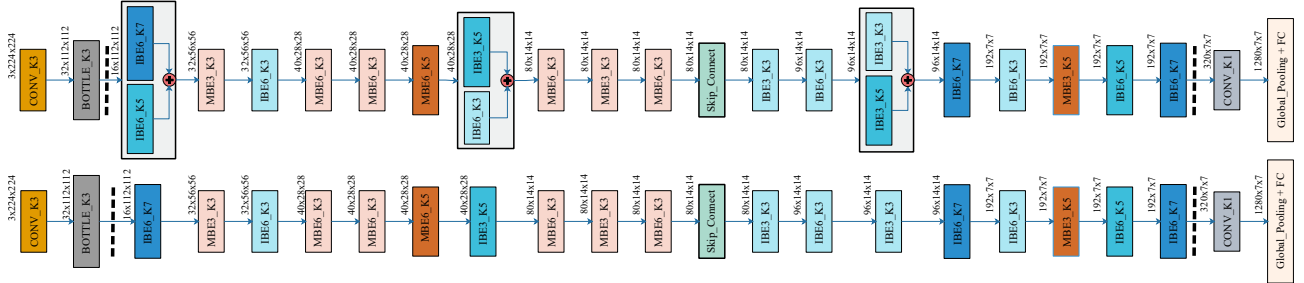


Figure 9. The Architecture of Fair DARTS-D (top) and C (bottom). IBEx\_Ky refers to an inverted bottleneck without an inset skip connection, while MBEx\_Ky is the one with it. BOTTLE\_K3 is the inverted bottleneck without expansion.

it's impossible to achieve this, as shown in Figure 5. At layer 11 only the skip connection operation is preferred, which cuts down the overall depth to 18.

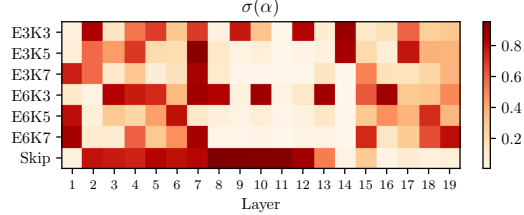


Figure 10. Heatmap of sigmoid values in the last searching epoch when running Fair DARTS in  $S_2$ . Many operations other than skip connections are also activated in parallel.

To be fair, we select at most two choices per layer if there are more than two above  $\sigma_{threshold}$  (0.75) and use the same training tricks as [27]. We exclude squeeze and excitation [11] and refrain from using AutoAugment [6] tricks though they can boost the classification accuracy further. The searched model FairDARTS-D is shown in Figure 9, which places the summation of two inverted bottleneck blocks nearby the down-sampling stage to keep more information. Moreover, it utilizes large kernels and big expansion blocks at the tail end. Furthermore, we raise the threshold (0.8) further to get a more lightweight model FairDARTS-C.

Recall in Section 3.2, we have predicted a promising case under cooperative settings in  $S_2$ . We count the number of dominant operations (above  $\sigma_{threshold}$ ) across this searching stage and exhibit its evolution on the right of Figure 1. In the beginning, no operations outperform above the threshold. Shortly later skip connections show obvious advantages. In the meantime, other operations are steadily optimized albeit a bit slower. In the end, they still exist cooperatively with skip connections, which verifies our assumption.

## 6. Ablation Studies and Analysis

### 6.1. Removing Skip Connections from $S_1$

As unfair advantages are mainly from skip connections, if we remove them from  $S_1$ , we should expect a fair play even in an exclusive competition. Several runs of this experiment also show that there is indeed no more prevailing operations that suppress others, including other parameterless ones like max-pooling and average pooling (Figure 11).

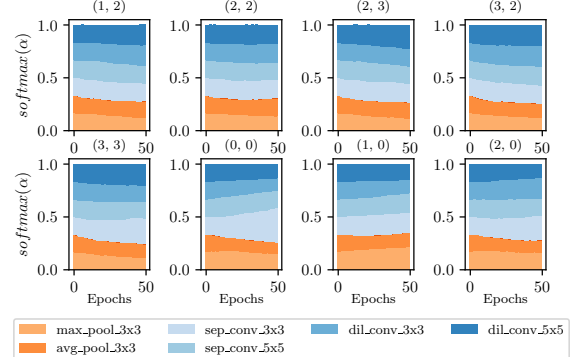


Figure 11. The softmax evolution where skip connections are removed from  $S_1$  when running DARTS on CIFAR-10. With unfair advantages removed, all operations enjoy a fair treatment.

### 6.2. How Does Zero-One Loss Matter?

**Removing Zero-One Loss.** We design two comparison groups for Fair DARTS with and without *zero-one loss*. All settings are kept the same. We count the distribution of the sigmoid outputs from architectural weights and plot it in Figure 12. The one without zero-one loss covers a wide range between 0 and 0.6. Whereas the proposed loss has narrowed the distribution into two modes around 0 and 1.

**Zero-One Loss Design.** We run two experiments on CIFAR-10, one with  $L_{0-1}$  (proposed) and the other  $L'_{0-1}$  (control). To some extent,  $L_{0-1}$  allows stepping out of local minimum while  $L'_{0-1}$  selects architectures only at an early stage which depends greatly on the initialization. This

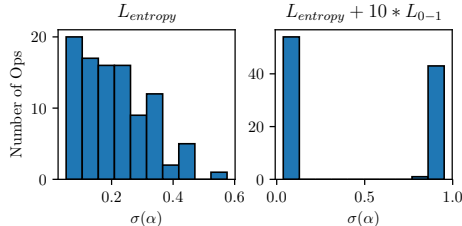


Figure 12. Histogram of sigmoid values in the last searching epoch without (left) and with  $L_{0-1}$  (right). On the right, this auxiliary loss has pushed the values towards 0 or 1.

matches our analysis in Section 4.2. The detailed results under both loss functions are shown in Figure 14.

**Loss Sensitivity.** As the weight  $w_{0-1}$  of this auxiliary loss goes higher, it should squeeze more operations towards two ends, but it must not overshadow the main entropy loss. We perform several experiments where an integer  $w_{0-1}$  varies within  $[0, 16]$ . Figure 13 shows the final number of dominant operations for each. We select a reasonable  $w_{0-1} = 10$  as it has the best trade-off.

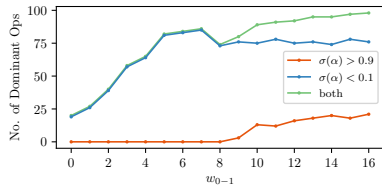


Figure 13. Number of dominant operations in the last searching epoch running Fair DARTS on CIFAR-10 w.r.t the sensitivity weight  $w_{0-1}$  of auxiliary loss  $L_{0-1}$ .

### 6.3. Discussion

We review the existing methods that seek to avoid the discussed weaknesses from a fairness perspective. In general, adding dropouts [5, 32] to operations is similar to blending them with a simple additive Gaussian noise, both reduce the performance gain from unfair advantages. Early-stopping [16] avoids the case before unfairness happens.

**Adding dropout to skip connections reduces unfairness.** The operation-level dropout [26] inserted after skip connections by PDARTS [5] can be viewed as an alleviation of unfair advantage. However, it comes with two obvious drawbacks. First, this dropout rate is hard to tune. Second, it is not so effective that they must involve another prior: setting the number of skip connections in the final cell to  $M$ . This is a very strong prior for searching good architectures [16].

**Adding dropout to all operations also helps.** Dropout troubles the training of skip connections and thus weakens the unfair advantage. Reasonably, higher dropout rates are more effective, especially for parameter-free operations.

Methods	CIFAR-10 Top-1 Acc (%)
Random (M=2)	$97.01 \pm 0.24$
Random (M=2, MultAdds $\geq 500M$ )	$97.14 \pm 0.28$
DARTS + Gaussian (cosine decay)	$97.12 \pm 0.23$

Table 4. **Experiment 1:** Random sampling (7 models each, averaged) from regularized search space ( $M = 2$ ). **Experiment 2:** Adding Gaussian noise to DARTS (repeated 3 times, averaged).

Therefore, RobustDARTS [32] adds dropout to all operations and obtains promising results.

**Early stopping matters.** DARTS+ [16] explicitly limits the maximum number of skip connections, which can be viewed as an early-stopping strategy nearby the previously mentioned *boundary epoch*, right before too many skip connections rise into power.

**Limiting the number of skip connections is a strong prior.** In the regularized search space of PDARTS [5] and DARTS+ [16], we find that simply by restricting  $M = 2$ , it is possible to generate competitive models even *without searching*. We randomly sample models from their search space and report the results in Table 4. In Experiment 1, the second group restricts the multiply-adds to be above 500M, to further leverage the average performance. Surprisingly, both groups outperform DARTS [18], whose best model has a top-1 accuracy  $97.00 \pm 0.14$ . All models are detailed in Table 10 and 11.

**Random noise can break unfair advantage.** Based on our theory, we can boldly postulate that adding a random noise also disrupts the unfair advantage. Therefore, on top of DARTS [18], we mix the skip connections’ architectural weights with a standard Gaussian noise  $\mathcal{N}(0, 1)$ , which has a cosine decay on 50 epochs. The results strongly confirm our hypothesis, as shown in Table 4. We repeat it for 3 times to have similar results. All models are detailed in Table 9.

## 7. Conclusion

We unveil two indispensable factors of the DARTS’s aggregation of excessive skip connections: **unfair advantages** and **exclusive competition**. We prove that breaking any one of them can improve the robustness. First, by allowing collaborative competition, each operation develops its architectural weight independently. In this regard, we achieve state-of-the-art performances both on CIFAR-10 and ImageNet. Second, disturbing the differential process with a Gaussian noise removes unfair advantage, whose results also compete with others. Meanwhile, the non-negligible discretization gap is reduced at maximum by coercing a novel auxiliary loss which polarizes the architectural weights.

One of our future works is to make it more memory-friendly. As Gumbel softmax is used to replace categorical distribution [29], is there a similar way to our approach?

More methods remain to be explored on our basis.

## References

[1] Gabriel Bender, Pieter-Jan Kindermans, Barret Zoph, Vijay Vasudevan, and Quoc Le. Understanding and Simplifying One-Shot Architecture Search. In *International Conference on Machine Learning*, pages 549–558, 2018.

[2] Kaifeng Bi, Changping Hu, Lingxi Xie, Xin Chen, Longhui Wei, and Qi Tian. Stabilizing DARTS with Amended Gradient Estimation on Architectural Parameters. *arXiv preprint arXiv:1910.11831*, 2019.

[3] Andrew Brock, Theodore Lim, James M Ritchie, and Nick Weston. SMASH: One-Shot Model Architecture Search through HyperNetworks. In *International Conference on Learning Representations*, 2018.

[4] Han Cai, Ligeng Zhu, and Song Han. ProxylessNAS: Direct Neural Architecture Search on Target Task and Hardware. In *International Conference on Learning Representations*, 2019.

[5] Xin Chen, Lingxi Xie, Jun Wu, and Qi Tian. Progressive Differentiable Architecture Search: Bridging the Depth Gap between Search and Evaluation. *International Conference on Computer Vision*, 2019.

[6] Ekin D Cubuk, Barret Zoph, Dandelion Mane, Vijay Vasudevan, and Quoc V Le. AutoAugment: Learning Augmentation Policies from Data. *arXiv preprint arXiv:1805.09501*, 2018.

[7] Xuanyi Dong and Yi Yang. One-Shot Neural Architecture Search via Self-Evaluated Template Network. In *Proceedings of the IEEE International Conference on Computer Vision*, pages 3681–3690, 2019.

[8] Xuanyi Dong and Yi Yang. Searching for a Robust Neural Architecture in Four GPU Hours. In *Proceedings of the IEEE Conference on Computer Vision and Pattern Recognition*, pages 1761–1770, 2019.

[9] Zichao Guo, Xiangyu Zhang, Haoyuan Mu, Wen Heng, Zechun Liu, Yichen Wei, and Jian Sun. Single Path One-Shot Neural Architecture Search with Uniform Sampling. *arXiv preprint arXiv:1904.00420*, 2019.

[10] Kaiming He, Xiangyu Zhang, Shaoqing Ren, and Jian Sun. Deep Residual Learning for Image Recognition. In *Proceedings of the IEEE conference on computer vision and pattern recognition*, pages 770–778, 2016.

[11] Jie Hu, Li Shen, and Gang Sun. Squeeze-and-Excitation Networks. In *Proceedings of the IEEE Conference on Computer Vision and Pattern Recognition*, pages 7132–7141, 2018.

[12] Eric Jang, Shixiang Gu, and Ben Poole. Categorical Reparameterization with Gumbel-Softmax. *International Conference on Learning Representations*, 2017.

[13] Guilin Li, Xing Zhang, Zitong Wang, Zhenguo Li, and Tong Zhang. StacNAS: Towards stable and consistent optimization for differentiable Neural Architecture Search. *arXiv preprint arXiv:1909.11926*, 2019.

[14] Liam Li and Ameet Talwalkar. Random Search and Reproducibility for Neural Architecture Search. *Conference on Uncertainty in Artificial Intelligence*, 2019.

[15] Yuanzhi Li and Yang Yuan. Convergence Analysis of Two-layer Neural Networks with Relu Activation. In *Advances in Neural Information Processing Systems*, pages 597–607, 2017.

[16] Hanwen Liang, Shifeng Zhang, Jiacheng Sun, Xingqiu He, Weiran Huang, Kechen Zhuang, and Zhenguo Li. DARTS+: Improved Differentiable Architecture Search with Early Stopping. *arXiv preprint arXiv:1909.06035*, 2019.

[17] Chenxi Liu, Barret Zoph, Maxim Neumann, Jonathon Shlens, Wei Hua, Li-Jia Li, Li Fei-Fei, Alan Yuille, Jonathan Huang, and Kevin Murphy. Progressive neural architecture search. In *Proceedings of the European Conference on Computer Vision (ECCV)*, pages 19–34, 2018.

[18] Hanxiao Liu, Karen Simonyan, and Yiming Yang. DARTS: Differentiable Architecture Search. In *International Conference on Learning Representations*, 2019.

[19] Zhichao Lu, Ian Whalen, Vishnu Boddeti, Yashesh Dhebar, Kalyanmoy Deb, Erik Goodman, and Wolfgang Banzhaf. NSGA-NET: A Multi-Objective Genetic Algorithm for Neural Architecture Search. In *Proceedings of the Genetic and Evolutionary Computation Conference*, pages 419–427, 2019.

[20] Chris J Maddison, Andriy Mnih, and Yee Whye Teh. The Concrete Distribution: A Continuous Relaxation of Discrete Random Variables. *International Conference on Learning Representations*, 2017.

[21] Niv Nayman, Asaf Noy, Tal Ridnik, Itamar Friedman, Rong Jin, and Lihi Zelnik-Manor. XNAS: Neural Architecture Search with Expert Advice. *arXiv preprint arXiv:1906.08031*, 2019.

[22] Hieu Pham, Melody Y Guan, Barret Zoph, Quoc V Le, and Jeff Dean. Efficient Neural Architecture Search via Parameter Sharing. In *International Conference on Machine Learning*, 2018.

[23] Esteban Real, Alok Aggarwal, Yanping Huang, and Quoc V Le. Regularized Evolution for Image Classifier Architecture Search. *International Conference on Machine Learning, AutoML Workshop*, 2018.

[24] Mark Sandler, Andrew Howard, Menglong Zhu, Andrey Zhmoginov, and Liang-Chieh Chen. MobileNetV2: Inverted Residuals and Linear Bottlenecks. In *Proceedings of the IEEE Conference on Computer Vision and Pattern Recognition*, pages 4510–4520, 2018.

[25] Christian Sciuto, Kaicheng Yu, Martin Jaggi, Claudiu Musat, and Mathieu Salzmann. Evaluating the Search Phase of Neural Architecture Search. *arXiv preprint arXiv:1902.08142*, 2019.

[26] Nitish Srivastava, Geoffrey Hinton, Alex Krizhevsky, Ilya Sutskever, and Ruslan Salakhutdinov. Dropout: A Simple Way to Prevent Neural Networks from Overfitting. *The Journal of Machine Learning Research*, 15(1):1929–1958, 2014.

[27] Mingxing Tan, Bo Chen, Ruoming Pang, Vijay Vasudevan, and Quoc V Le. MnasNet: Platform-Aware Neural Architecture Search for Mobile. In *Proceedings of the IEEE Conference on Computer Vision and Pattern Recognition*, 2019.

[28] Mingxing Tan and Quoc V Le. EfficientNet: Rethinking Model Scaling for Convolutional Neural Networks. In *International Conference on Machine Learning*, 2019.

[29] Bichen Wu, Xiaoliang Dai, Peizhao Zhang, Yanghan Wang, Fei Sun, Yiming Wu, Yuandong Tian, Peter Vajda, Yangqing

Jia, and Kurt Keutzer. FBNet: Hardware-Aware Efficient ConvNet Design via Differentiable Neural Architecture Search. In *Proceedings of the IEEE Conference on Computer Vision and Pattern Recognition*, 2019.

- [30] Sirui Xie, Hehui Zheng, Chunxiao Liu, and Liang Lin. SNAS: Stochastic Neural Architecture Search. *International Conference on Learning Representations*, 2019.
- [31] Yuhui Xu, Lingxi Xie, Xiaopeng Zhang, Xin Chen, Guo-Jun Qi, Qi Tian, and Hongkai Xiong. PC-DARTS: Partial Channel Connections for Memory-efficient Differentiable Architecture Search. *arXiv preprint arXiv:1907.05737*, 2019.
- [32] Arber Zela, Thomas Elsken, Tommoy Saikia, Yassine Marakchi, Thomas Brox, and Frank Hutter. Understanding and Robustifying Differentiable Architecture Search. *arXiv preprint arXiv:1909.09656*, 2019.
- [33] Xiawu Zheng, Rongrong Ji, Lang Tang, Baochang Zhang, Jianzhuang Liu, and Qi Tian. Multinomial Distribution Learning for Effective Neural Architecture Search. *International Conference on Computer Vision*, 2019.
- [34] Barret Zoph and Quoc V Le. Neural Architecture Search with Reinforcement Learning. In *International Conference on Learning Representations*, 2017.
- [35] Barret Zoph, Vijay Vasudevan, Jonathon Shlens, and Quoc V Le. Learning Transferable Architectures for Scalable Image Recognition. In *Proceedings of the IEEE Conference on Computer Vision and Pattern Recognition*, volume 2, 2018.

## A. Weight-sharing Neural Architecture Search

Weight-sharing in neural architecture search is now prominent because of its efficiency [3, 22, 1, 9]. They can roughly be divided into two categories.

**One-stage approaches.** Specifically, ENAS [22] adopts a reinforced approach to train a controller to sample subnetworks from the supernet. ‘Good’ subnetworks yield high rewards so that the final policy of the controller is able to find competitive ones. Notice the controller and subnetworks are trained alternatively. DARTS [18] and many of its variants [29, 30, 8, 5] are also a nested optimization based on weight-sharing but in a differentiable way. Besides, DARTS creates an exclusive competition by selecting only one operation on an edge, opposed to ENAS where more operations can be activated at the same time.

**Two-stage approaches.** There are some other weight-sharing methods who use the trained supernet as an evaluator [3, 1, 9]. We need to make a distinction here as DARTS is a one-stage approach. The supernet of DARTS is meant to learn towards a single solution, where other paths are less valued (weighted). Instead like in [9], all paths are uniformly sampled, so to give an equal importance on selected paths. As the supernet is used for different purposes, two-stage approaches should be singled out for discussion in this paper.

## B. Search Spaces

There are two search spaces extensively adopted in recent NAS approaches. The one DARTS proposed, we denote as  $S_1$ , is cell-based with flexible inner connections [18, 5], and the other  $S_2$  is at the block level of the entire network [27, 4, 29]. We use the term *proxy* and *proxyless* to differentiate whether it directly represents the backbone architecture. Our experiments cover both categories, if otherwise explicitly written, the first is searched on CIFAR-10 and the second on ImageNet.

**Search Space  $S_1$ .** Our first search space  $S_1$  follows DARTS [18] with an exception of excluding the *zero operation*, as done in [32]. Namely,  $S_1$  works in the previously mentioned DAG of  $N = 7$  nodes, first two nodes are the outputs of last two cells  $c_{k-1}$  and  $c_{k-2}$ , four intermediate nodes with each has incoming edges from the former nodes. The output node of DAG is a concatenation of all intermediate nodes. Each edge contains 7 candidate operations:

- max\_pool\_3x3, avg\_pool\_3x3, skip\_connect,
- sep\_conv\_3x3, sep\_conv\_5x5,
- dil\_conv\_3x3, dil\_conv\_5x5.

**Search Space  $S_2$ .** The second search space  $S_2$  is similar to that of ProxylessNAS [4] which uses MobileNetV2 [24]

as its backbone. We make several essential modifications. Specifically, there are  $L = 19$  layers and each contains  $N = 7$  following choices,

- Inverted bottlenecks with an expansion rate  $x$  in (3,6), a kernel size  $y$  in (3,5,7), later referred to as  $ExKy$ ,
- skip connection.

## C. Experiment Details

The list of all experiments we perform for this paper are summarized in Table 5.

To summarize, we run DARTS [18] in  $S_1$  and  $S_2$ , confirming the aggregation of skip connections in both search spaces. We also show the large discretization gap in  $S_2$ .

In comparison, we run Fair DARTS in  $S_1$  and  $S_2$  to show their differences. First, the number of skip connections is largely reduced in  $S_1$ , see Figure 8 (main text). Second, Figure 16 (supplementary) exhibit the final heatmap of architectural weights  $\sigma$  where skip connections coexist with other operations, meantime, the values of  $\sigma$  are also close to 0 or 1, which can minimize the discretization gap.

### C.1. Search on CIFAR-10 in Search Space $S_1$

We initialize all architectural weights to  $0^7$  and set  $w_{0-1} = 10$ . We comply with the same hyperparameters with some exceptions: a batch size 128, learning rate 0.005, and Adam optimizer with a decay of 3e-3 and beta (0.9, 0.999). Moreover, we comply with the same strategy of grouping training and validation data as [18]. The edge correspondence in search space  $S_1$  is given in Table 6. We also use the first-order optimization to save time.

### C.2. Search on ImageNet in Search Space $S_2$

We use the SGD optimizer with an initial learning rate 0.02 (cosine decayed by epochs) for the network weights and Adam optimizer with 5e-4 for architectural weights. Besides, we set  $\sigma_{threshold} = 0.75$  and  $w_{0-1} = 1.0$ .

There is a minor issue need to concern. The innate *skip connections* are removed from inverted bottlenecks since skip connections have already been made a parallel choice in our search space.

## C.3. Zero-one Loss Comparison

Figure 14 compares results on two different loss designs. With the proposed loss function  $L_{0-1}$  so that Fair DARTS is less subjective to initialization. The sigmoid values reach to their optima more slowly than that of  $L'_{0-1}$ . It also gives a fair opportunity near 0.5, the  $3 \times 3$  dilation convolution on Edge (3,4) first increases and then decreases, which matches the second criteria of loss design.

<sup>7</sup>Its sigmoid output is 0.5 (fair starting point).

Index	Method	Search Space	Loss	Optimization	Figure <sup>†</sup>	Figure <sup>‡</sup>	Table <sup>‡</sup>
1	DARTS*	$S_1$	$\mathcal{L}_{val}$	Bi-level	2,3,4	18,22	
2	DARTS	$S_2$	$\mathcal{L}_{val}$	Bi-level	1,5		
3	Fair DARTS	$S_1$	$\mathcal{L}_{val}$	Bi-level	12		
4	Fair DARTS*	$S_1$	$\mathcal{L}_{val} + w_{0-1} L_{0-1}$	Bi-level	13		
5	Fair DARTS*	$S_1$	$\mathcal{L}_{val} + 10 * L'_{0-1}$	Bi-level	7,8,12	15,16,17,21,23	8
6	Fair DARTS	$S_1$	$\mathcal{L}_{val} + 10 * L'_{0-1}$	Bi-level		14,19	
7	Fair DARTS	$S_1$	$\mathcal{L}_{val} + 10 * L_{0-1}$	Single-level		15,20	
8	Fair DARTS	$S_2$	$\mathcal{L}_{val} + 10 * L_{0-1}$	Bi-level	1,10,9		
9	DARTS	$S_1 - \{\text{skip connections}\}$	$\mathcal{L}_{val}$	Bi-level	11	24	
10	Random	$S_1 + \{\text{priors for skips}\}$	n/a	n/a			10
11	Random	$S_1 + \{\text{priors for skips}\} + \{\text{flops} \geq 500M\}$	n/a	n/a			11
12	Noise*	$S_1 + \{\mathcal{N}(0, 1)\}$	$\mathcal{L}_{val}$	Bi-level			9

Table 5. All experiments conducted for this paper. By default,  $S_1$  is for CIFAR-10,  $S_2$  for ImageNet. Note  $\mathcal{L}_{val}$  refers to  $\mathcal{L}_{val}(w^*(\alpha), \alpha)$ .  
<sup>†</sup>: Main text. <sup>‡</sup>: In the appendix. \*:run  $k = 4$  times, \*:  $w_{0-1} \in \text{range}(16)$ .

Edge	$(j, k)$
0	$(0, 0)$
1	$(0, 1)$
2	$(1, 0)$
3	$(1, 1)$
4	$(1, 2)$
5	$(2, 0)$
6	$(2, 1)$
7	$(2, 2)$
8	$(2, 3)$
9	$(3, 0)$
10	$(3, 1)$
11	$(3, 2)$
12	$(3, 3)$
13	$(3, 4)$

Table 6. Edge correspondence in  $S_1$ . Edge  $i$  is represented as a pair  $(i, j)$  where  $j$  is counted from intermediate nodes and  $k$  from previous cell outputs. See Figure 25 for further details.

Mothods	Skip Connection	Other Ops
DARTS [18]	No Drop	No Drop
PDARTS [5]	Drop	No Drop
RobustDARTS [32]	Drop	Drop

Table 7. Dropout strategies of DARTS variants .

#### C.4. Single-level vs. Bi-level Optimization

The  $5 \times 5$  separable convolution on edge  $(2, 2)$  under bi-level setting weighs higher at the early stage but much decreased in the end, which can be viewed as robustness to a local optimum. See Figure 15.

#### D. Figures on Architectural Weights

Figure 18 and 22 gives the complete *softmax* evolution when running DARTS on CIFAR-10 in  $S_1$ . Figure 24 is a similar case except the skip connection is removed.

Figure 19 gives the complete *sigmoid* evolution when running Fair DARTS on CIFAR-10 in  $S_1$  with  $L'_{0-1}$ .

Figure 20, 21 gives the complete sigmoid evolution

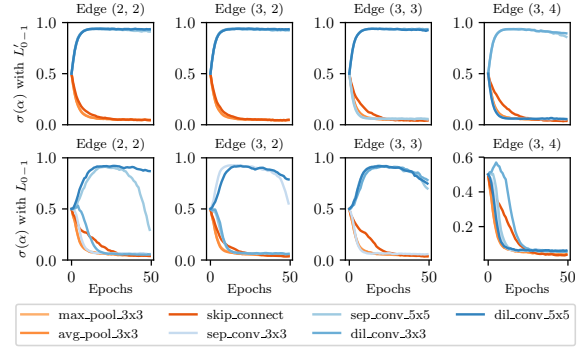


Figure 14. Comparison of sigmoid evolution when running Fair DARTS with  $L'_{0-1}$  (top) and  $L_{0-1}$  (bottom) in  $S_1$ . With the proposed loss at the bottom, sigmoid values manage to step out of local optima.

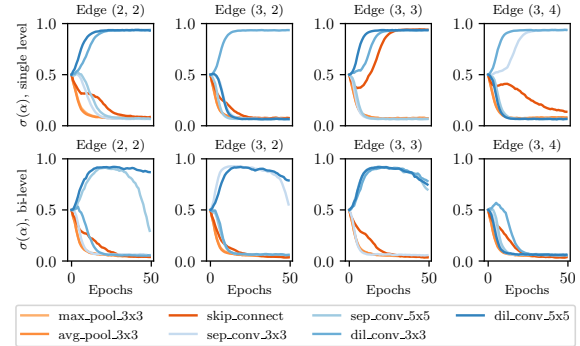


Figure 15. Comparison of sigmoid evolution when running Fair DARTS with single and bi-level optimization. Bi-level has better robustness to local minimum.

when running Fair DARTS on CIFAR-10 in  $S_1$  with *single-level* and *bi-level* optimization respectively. Figure 23 is a stacked-bar version of Figure 21.

Model	Architecture Genotype
FairDARTS-b	Genotype(normal=[('sep_conv_3x3', 2, 0), ('sep_conv_3x3', 2, 1), ('sep_conv_3x3', 3, 1), ('dil_conv_3x3', 4, 0), ('sep_conv_5x5', 4, 1), ('dil_conv_5x5', 5, 1)], normal_concat=range(2, 6), reduce=[('skip_connect', 2, 0), ('dil_conv_3x3', 2, 1), ('skip_connect', 3, 0), ('dil_conv_3x3', 3, 1), ('max_pool_3x3', 4, 0), ('sep_conv_3x3', 4, 1), ('skip_connect', 5, 2), ('max_pool_3x3', 5, 0)], reduce_concat=range(2, 6))
FairDARTS-c	Genotype(normal=[('max_pool_3x3', 2, 0), ('sep_conv_5x5', 2, 1), ('dil_conv_3x3', 4, 0), ('dil_conv_5x5', 4, 2), ('skip_connect', 5, 3), ('sep_conv_3x3', 5, 0)], normal_concat=range(2, 6), reduce=[('dil_conv_3x3', 2, 1), ('dil_conv_5x5', 2, 0), ('dil_conv_3x3', 3, 0), ('sep_conv_3x3', 3, 1), ('sep_conv_5x5', 4, 0), ('sep_conv_5x5', 4, 3), ('sep_conv_5x5', 5, 0), ('skip_connect', 5, 1)], reduce_concat=range(2, 6))
FairDARTS-d	Genotype(normal=[('sep_conv_3x3', 2, 0), ('sep_conv_5x5', 2, 1), ('dil_conv_3x3', 3, 1), ('max_pool_3x3', 3, 0), ('dil_conv_3x3', 4, 0), ('dil_conv_3x3', 4, 1), ('sep_conv_3x3', 5, 0), ('dil_conv_5x5', 5, 1)], normal_concat=range(2, 6), reduce=[('max_pool_3x3', 2, 0), ('sep_conv_5x5', 2, 1), ('avg_pool_3x3', 3, 0), ('dil_conv_5x5', 3, 2), ('dil_conv_3x3', 4, 3), ('avg_pool_3x3', 4, 0), ('avg_pool_3x3', 5, 0), ('skip_connect', 5, 3)], reduce_concat=range(2, 6))
FairDARTS-e	Genotype(normal=[('sep_conv_3x3', 2, 0), ('sep_conv_3x3', 2, 1), ('dil_conv_3x3', 4, 1), ('dil_conv_3x3', 4, 2), ('dil_conv_3x3', 5, 0), ('dil_conv_5x5', 5, 1)], normal_concat=range(2, 6), reduce=[('max_pool_3x3', 2, 1), ('max_pool_3x3', 2, 0), ('max_pool_3x3', 3, 1), ('max_pool_3x3', 3, 0), ('sep_conv_5x5', 4, 1), ('max_pool_3x3', 4, 0), ('avg_pool_3x3', 5, 0), ('dil_conv_5x5', 5, 1)], reduce_concat=range(2, 6))
FairDARTS-f	Genotype(normal=[('max_pool_3x3', 2, 0), ('sep_conv_3x3', 2, 1), ('dil_conv_3x3', 3, 1), ('sep_conv_5x5', 4, 1), ('sep_conv_3x3', 5, 0), ('sep_conv_3x3', 5, 1)], normal_concat=range(2, 6), reduce=[('max_pool_3x3', 2, 0), ('max_pool_3x3', 2, 1), ('max_pool_3x3', 3, 0), ('dil_conv_3x3', 3, 1), ('dil_conv_3x3', 4, 2), ('max_pool_3x3', 4, 0), ('max_pool_3x3', 5, 0), ('sep_conv_3x3', 5, 1)], reduce_concat=range(2, 6))
FairDARTS-g	Genotype(normal=[('sep_conv_3x3', 2, 0), ('sep_conv_3x3', 2, 1), ('skip_connect', 4, 3), ('sep_conv_5x5', 4, 1), ('dil_conv_3x3', 5, 0), ('sep_conv_3x3', 5, 1)], normal_concat=range(2, 6), reduce=[('avg_pool_3x3', 2, 1), ('skip_connect', 2, 0), ('skip_connect', 3, 2), ('max_pool_3x3', 3, 1), ('sep_conv_5x5', 4, 3), ('max_pool_3x3', 4, 0), ('dil_conv_3x3', 5, 1), ('dil_conv_3x3', 5, 4)], reduce_concat=range(2, 6))

Table 8. Fair DARTS architecture genotypes. FairDARTS-a is not included here since it is already drawn in Figure 7 (main text).

Model	Architecture Genotype
0	Genotype(normal=[('sep_conv_3x3', 1), ('sep_conv_3x3', 0), ('dil_conv_5x5', 1), ('dil_conv_3x3', 2), ('sep_conv_3x3', 1), ('dil_conv_5x5', 3), ('dil_conv_5x5', 4), ('dil_conv_3x3', 3)], normal_concat=range(2, 6), reduce=[('max_pool_3x3', 0), ('max_pool_3x3', 1), ('avg_pool_3x3', 0), ('dil_conv_5x5', 2), ('skip_connect', 1), ('max_pool_3x3', 0), ('skip_connect', 3), ('avg_pool_3x3', 1)], reduce_concat=range(2, 6))
1	Genotype(normal=[('dil_conv_3x3', 1), ('sep_conv_3x3', 0), ('dil_conv_3x3', 2), ('dil_conv_3x3', 1), ('sep_conv_3x3', 1), ('dil_conv_5x5', 3), ('dil_conv_3x3', 3), ('dil_conv_5x5', 4)], normal_concat=range(2, 6), reduce=[('dil_conv_5x5', 1), ('skip_connect', 0), ('max_pool_3x3', 0), ('dil_conv_3x3', 2), ('skip_connect', 3), ('skip_connect', 2), ('skip_connect', 3)], reduce_concat=range(2, 6))
2	Genotype(normal=[('dil_conv_3x3', 1), ('skip_connect', 0), ('sep_conv_3x3', 1), ('dil_conv_3x3', 2), ('sep_conv_3x3', 1), ('dil_conv_3x3', 2), ('dil_conv_5x5', 4), ('dil_conv_5x5', 1)], normal_concat=range(2, 6), reduce=[('max_pool_3x3', 1), ('max_pool_3x3', 0), ('avg_pool_3x3', 0), ('dil_conv_5x5', 2), ('avg_pool_3x3', 1), ('skip_connect', 2), ('skip_connect', 3), ('skip_connect', 2)], reduce_concat=range(2, 6))

Table 9. Architecture genotypes when adding Gaussian noise to DARTS. Discussed in Section 6.3 (main text).

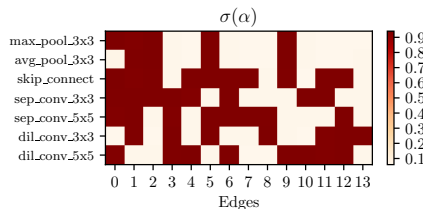


Figure 16. Heatmap of  $\sigma(\alpha)$  in the last epoch when searching with Fair DARTS on CIFAR-10 (in  $S_1$ ). As a result of the sigmoid feature and the auxiliary loss  $L_{0-1}$ , the values are mainly around 0 and 1.

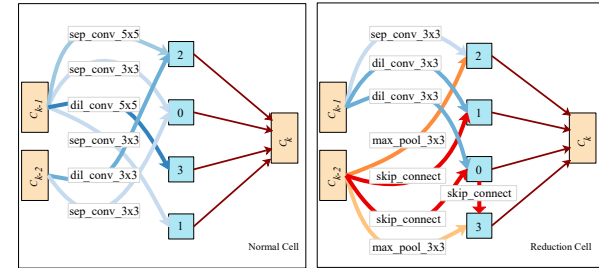


Figure 17. FairDARTS-b cells searched on CIFAR-10 in  $S_1$ .

## E. More Discussions

Despite superficially irrelevant, Insight 1 and 2 are somewhat twined. As the former focuses on the reason for excess-

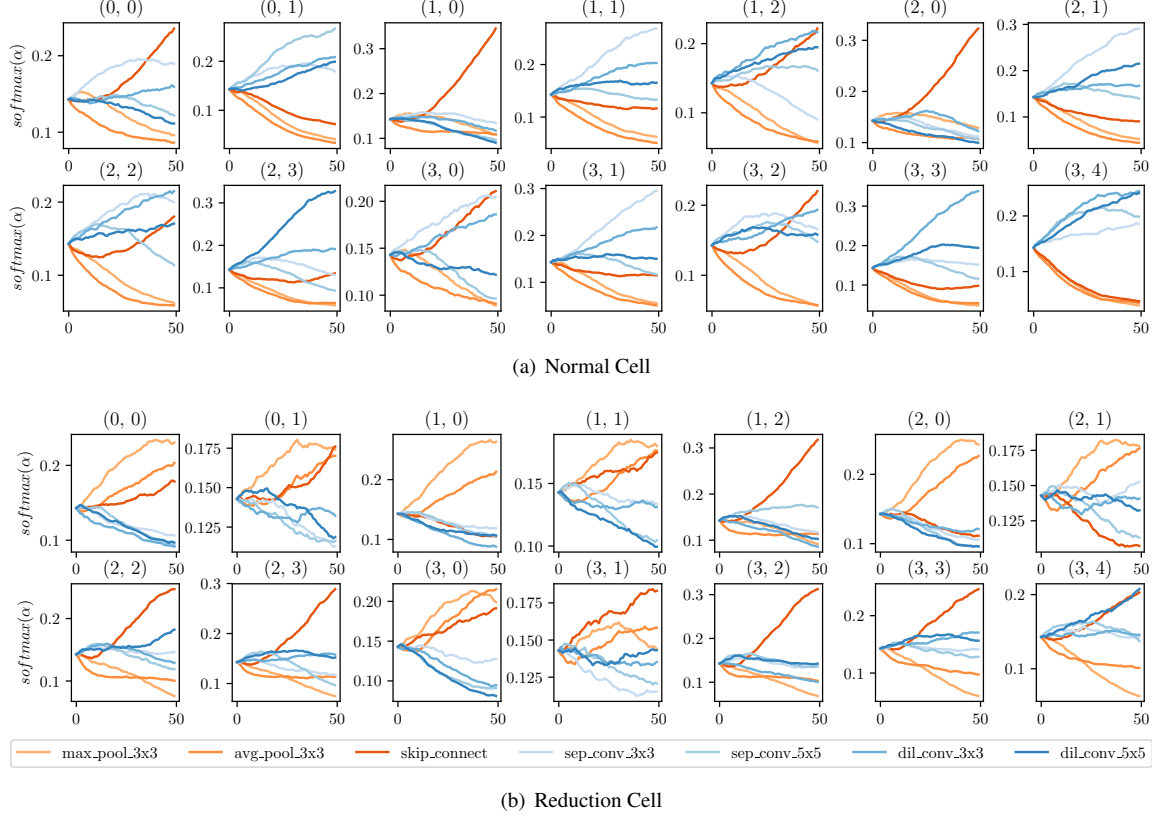
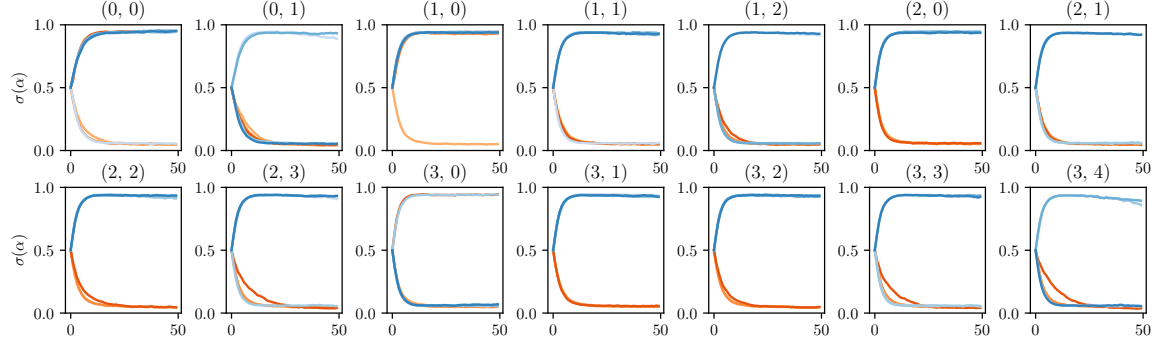


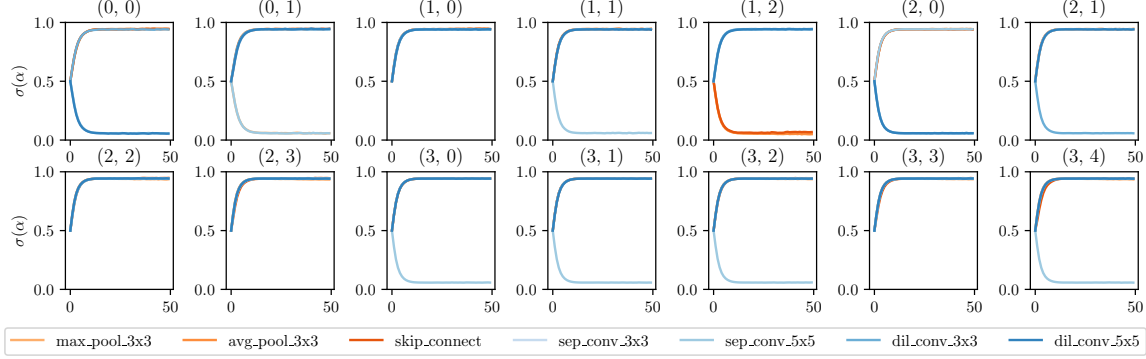
Figure 18. The softmax evolution when running DARTS on CIFAR-10 in  $S_1$  ( $k = 3$ ).

Model	Architecture Genotype
0	Genotype(normal=[('skip_connect', 1), ('sep_conv_5x5', 0), ('skip_connect', 1), ('dil_conv_5x5', 0), ('avg_pool_3x3', 1), ('dil_conv_3x3', 0), ('max_pool_3x3', 0), ('sep_conv_3x3', 3)], normal.concat=range(2, 6), reduce=[('dil_conv_3x3', 1), ('dil_conv_5x5', 0), ('max_pool_3x3', 1), ('dil_conv_5x5', 2), ('skip_connect', 0), ('dil_conv_3x3', 1), ('avg_pool_3x3', 4), ('sep_conv_5x5', 1)], reduce_concat=range(2, 6))
1	Genotype(normal=[('skip_connect', 1), ('skip_connect', 0), ('dil_conv_3x3', 0), ('sep_conv_5x5', 2), ('dil_conv_5x5', 1), ('sep_conv_5x5', 3), ('dil_conv_3x3', 3), ('max_pool_3x3', 4)], normal.concat=range(2, 6), reduce=[('sep_conv_3x3', 1), ('sep_conv_3x3', 0), ('dil_conv_3x3', 2), ('max_pool_3x3', 1), ('sep_conv_3x3', 0), ('sep_conv_3x3', 1), ('max_pool_3x3', 2), ('skip_connect', 3)], reduce_concat=range(2, 6))
2	Genotype(normal=[('avg_pool_3x3', 0), ('skip_connect', 1), ('dil_conv_5x5', 0), ('dil_conv_3x3', 2), ('sep_conv_5x5', 2), ('skip_connect', 3), ('avg_pool_3x3', 1), ('avg_pool_3x3', 4)], normal.concat=range(2, 6), reduce=[('avg_pool_3x3', 0), ('avg_pool_3x3', 1), ('avg_pool_3x3', 0), ('sep_conv_5x5', 1), ('sep_conv_3x3', 2), ('avg_pool_3x3', 1), ('sep_conv_3x3', 2), ('max_pool_3x3', 1)], reduce_concat=range(2, 6))
3	Genotype(normal=[('skip_connect', 1), ('dil_conv_3x3', 0), ('sep_conv_3x3', 0), ('avg_pool_3x3', 2), ('dil_conv_5x5', 0), ('dil_conv_3x3', 3), ('max_pool_3x3', 1), ('skip_connect', 4)], normal.concat=range(2, 6), reduce=[('dil_conv_3x3', 0), ('sep_conv_5x5', 1), ('sep_conv_5x5', 1), ('sep_conv_5x5', 0), ('avg_pool_3x3', 0), ('sep_conv_5x5', 2), ('sep_conv_3x3', 0), ('max_pool_3x3', 1)], reduce_concat=range(2, 6))
4	Genotype(normal=[('dil_conv_5x5', 1), ('skip_connect', 0), ('sep_conv_5x5', 0), ('skip_connect', 2), ('sep_conv_5x5', 3), ('dil_conv_5x5', 2), ('avg_pool_3x3', 0), ('max_pool_3x3', 3)], normal.concat=range(2, 6), reduce=[('dil_conv_3x3', 0), ('dil_conv_3x3', 1), ('max_pool_3x3', 0), ('avg_pool_3x3', 2), ('max_pool_3x3', 0), ('avg_pool_3x3', 2), ('dil_conv_3x3', 0), ('dil_conv_3x3', 2)], reduce_concat=range(2, 6))
5	Genotype(normal=[('sep_conv_5x5', 0), ('skip_connect', 1), ('sep_conv_3x3', 2), ('sep_conv_3x3', 0), ('avg_pool_3x3', 2), ('skip_connect', 0), ('sep_conv_3x3', 0), ('dil_conv_5x5', 3)], normal.concat=range(2, 6), reduce=[('avg_pool_3x3', 1), ('sep_conv_5x5', 0), ('dil_conv_3x3', 2), ('skip_connect', 1), ('avg_pool_3x3', 2), ('skip_connect', 1), ('sep_conv_3x3', 4), ('dil_conv_3x3', 1)], reduce_concat=range(2, 6))
6	Genotype(normal=[('skip_connect', 1), ('sep_conv_5x5', 0), ('max_pool_3x3', 0), ('dil_conv_3x3', 1), ('sep_conv_5x5', 1), ('avg_pool_3x3', 0), ('skip_connect', 4), ('sep_conv_5x5', 0)], normal.concat=range(2, 6), reduce=[('dil_conv_5x5', 1), ('sep_conv_3x3', 0), ('sep_conv_5x5', 0), ('dil_conv_5x5', 1), ('max_pool_3x3', 1), ('max_pool_3x3', 3), ('dil_conv_5x5', 2), ('max_pool_3x3', 1)], reduce_concat=range(2, 6))

Table 10. Randomly sampled architecture genotypes in  $S_1$  setting  $M = 2$ . Discussed in Section 6.3 (main text).



(a) Normal Cell



(b) Reduction Cell

Figure 19. The sigmoid evolution when running Fair DARTS with  $L'_{0-1}$  loss in  $S_1$ .

sive skip connections, the latter addresses approximations in the transformation chain:  $D_{discrete} \rightarrow C_{continuous} \rightarrow D'_{discrete}$ . It is important to notice the discretization from  $C$  to  $D'$  is ill-conditioned, where a poor approximation leads to large inconsistency between the over-parameterized network (supernet) and the derived standalone model. If there is a proper transformation from  $C$  to  $D'$ , an excessive number of skip connections can be easily spotted (architectural weights close to 1). Particularly, a supernet with too many skip connections is high in loss. Simple optimization tricks can be utilized to step out such a poor solution with high loss, which in turn alleviates the situation in Insight 1.

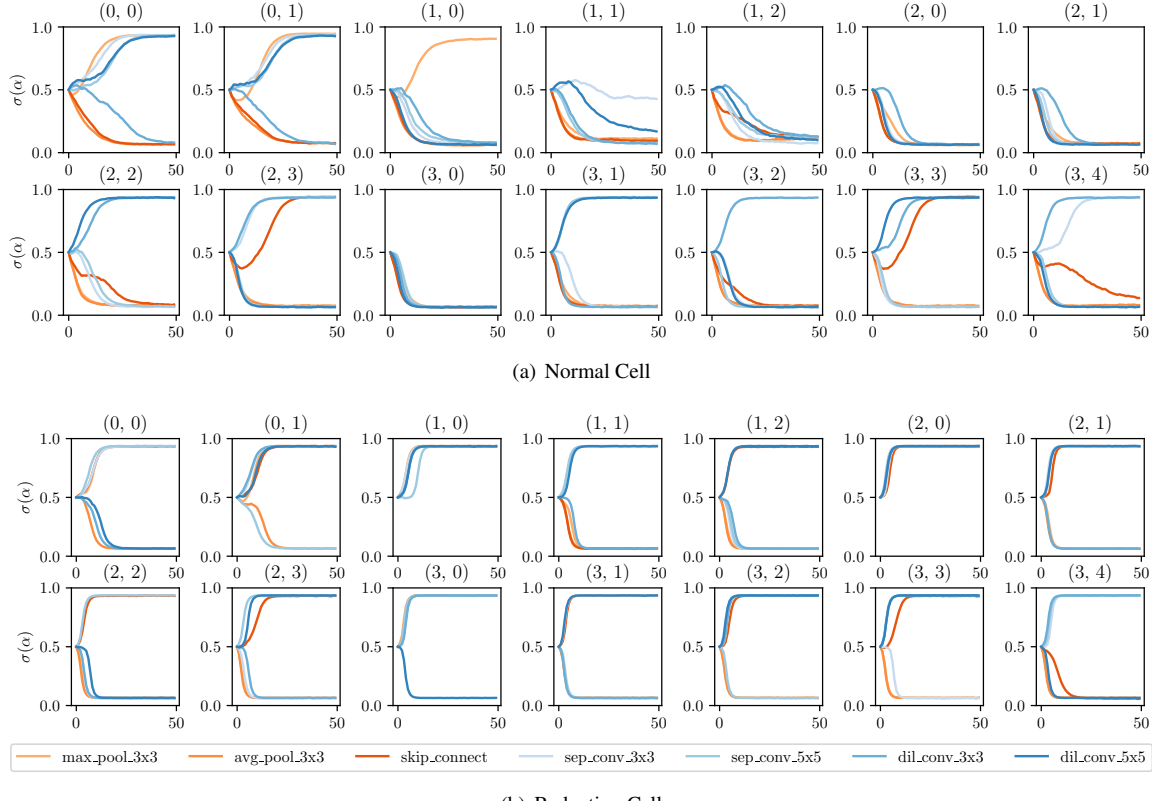


Figure 20. The sigmoid evolution when running Fair DARTS with single-level optimization in  $S_1$ .

Model	Architecture Genotype
0	Genotype(normal=[('skip_connect', 1), ('sep_conv_3x3', 0), ('skip_connect', 0), ('dil_conv_3x3', 2), ('sep_conv_3x3', 1), ('dil_conv_5x5', 2), ('sep_conv_3x3', 2), ('dil_conv_5x5', 1)], normal_concat=range(2, 6), reduce=[('skip_connect', 0), ('sep_conv_5x5', 1), ('avg_pool_3x3', 2), ('dil_conv_5x5', 0), ('sep_conv_3x3', 0), ('dil_conv_5x5', 2), ('sep_conv_5x5', 1), ('dil_conv_5x5', 2)], reduce_concat=range(2, 6))
1	Genotype(normal=[('dil_conv_3x3', 0), ('sep_conv_3x3', 1), ('skip_connect', 2), ('skip_connect', 1), ('sep_conv_5x5', 0), ('dil_conv_3x3', 1), ('sep_conv_5x5', 1), ('dil_conv_5x5', 4)], normal_concat=range(2, 6), reduce=[('dil_conv_3x3', 0), ('dil_conv_3x3', 1), ('avg_pool_3x3', 1), ('skip_connect', 0), ('dil_conv_5x5', 1), ('skip_connect', 3), ('skip_connect', 0), ('max_pool_3x3', 3)], reduce_concat=range(2, 6))
2	Genotype(normal=[('sep_conv_5x5', 0), ('max_pool_3x3', 1), ('sep_conv_5x5', 1), ('skip_connect', 0), ('skip_connect', 2), ('max_pool_3x3', 1), ('sep_conv_5x5', 3), ('sep_conv_3x3', 2)], normal_concat=range(2, 6), reduce=[('sep_conv_5x5', 0), ('skip_connect', 1), ('max_pool_3x3', 1), ('sep_conv_5x5', 2), ('dil_conv_5x5', 3), ('max_pool_3x3', 0), ('dil_conv_3x3', 1), ('max_pool_3x3', 2)], reduce_concat=range(2, 6))
3	Genotype(normal=[('sep_conv_3x3', 0), ('max_pool_3x3', 1), ('dil_conv_5x5', 2), ('dil_conv_5x5', 0), ('sep_conv_5x5', 3), ('sep_conv_5x5', 0), ('skip_connect', 3), ('skip_connect', 0)], normal_concat=range(2, 6), reduce=[('avg_pool_3x3', 0), ('sep_conv_5x5', 1), ('avg_pool_3x3', 1), ('dil_conv_3x3', 0), ('dil_conv_5x5', 3), ('sep_conv_5x5', 2), ('avg_pool_3x3', 1), ('dil_conv_5x5', 4)], reduce_concat=range(2, 6))
4	Genotype(normal=[('dil_conv_5x5', 0), ('sep_conv_5x5', 1), ('sep_conv_3x3', 2), ('skip_connect', 0), ('sep_conv_5x5', 3), ('sep_conv_5x5', 0), ('avg_pool_3x3', 1), ('skip_connect', 0)], normal_concat=range(2, 6), reduce=[('max_pool_3x3', 1), ('skip_connect', 0), ('dil_conv_5x5', 1), ('dil_conv_5x5', 2), ('sep_conv_5x5', 0), ('sep_conv_3x3', 1), ('avg_pool_3x3', 1), ('skip_connect', 0)], reduce_concat=range(2, 6))
5	Genotype(normal=[('sep_conv_5x5', 1), ('sep_conv_5x5', 0), ('skip_connect', 2), ('sep_conv_3x3', 0), ('dil_conv_5x5', 2), ('dil_conv_3x3', 3), ('max_pool_3x3', 0), ('skip_connect', 2)], normal_concat=range(2, 6), reduce=[('max_pool_3x3', 0), ('dil_conv_5x5', 1), ('max_pool_3x3', 2), ('skip_connect', 0), ('dil_conv_5x5', 0), ('sep_conv_5x5', 3), ('sep_conv_3x3', 1), ('dil_conv_5x5', 3)], reduce_concat=range(2, 6))
6	Genotype(normal=[('avg_pool_3x3', 0), ('sep_conv_5x5', 1), ('sep_conv_5x5', 0), ('skip_connect', 1), ('dil_conv_5x5', 0), ('sep_conv_5x5', 1), ('skip_connect', 4), ('sep_conv_5x5', 0)], normal_concat=range(2, 6), reduce=[('dil_conv_5x5', 1), ('avg_pool_3x3', 0), ('avg_pool_3x3', 2), ('sep_conv_5x5', 0), ('max_pool_3x3', 0), ('dil_conv_5x5', 2), ('sep_conv_5x5', 3), ('skip_connect', 0)], reduce_concat=range(2, 6))

Table 11. Randomly sampled architecture genotypes in  $S_1$  setting  $M = 2$  and multiply-adds  $> 500M$ . Discussed in Section 6.3 (main text).

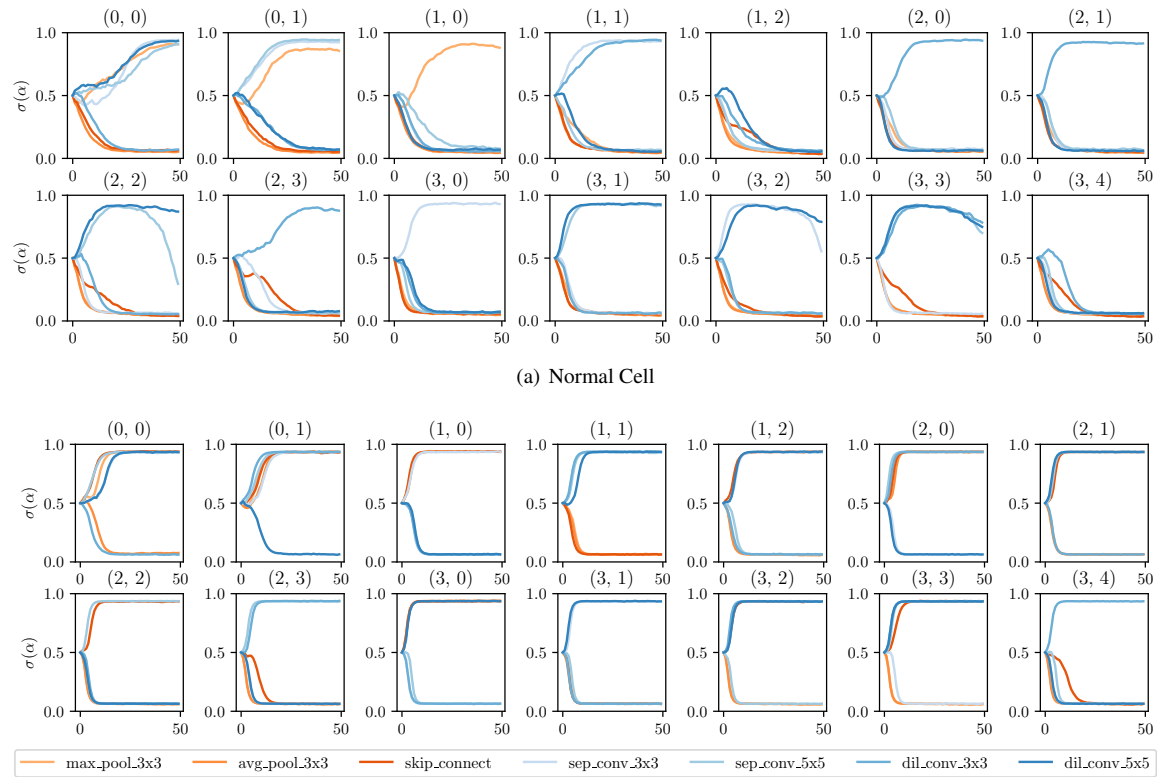
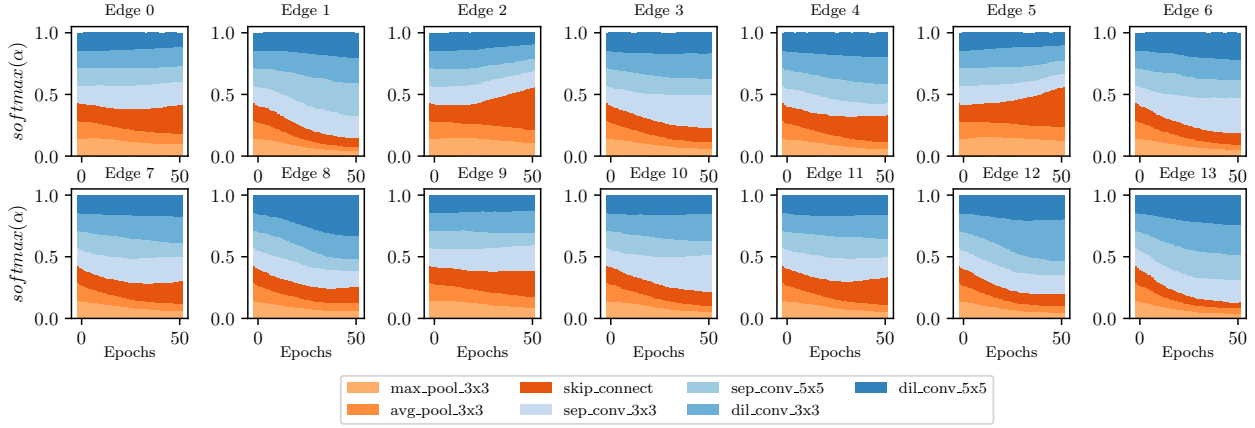
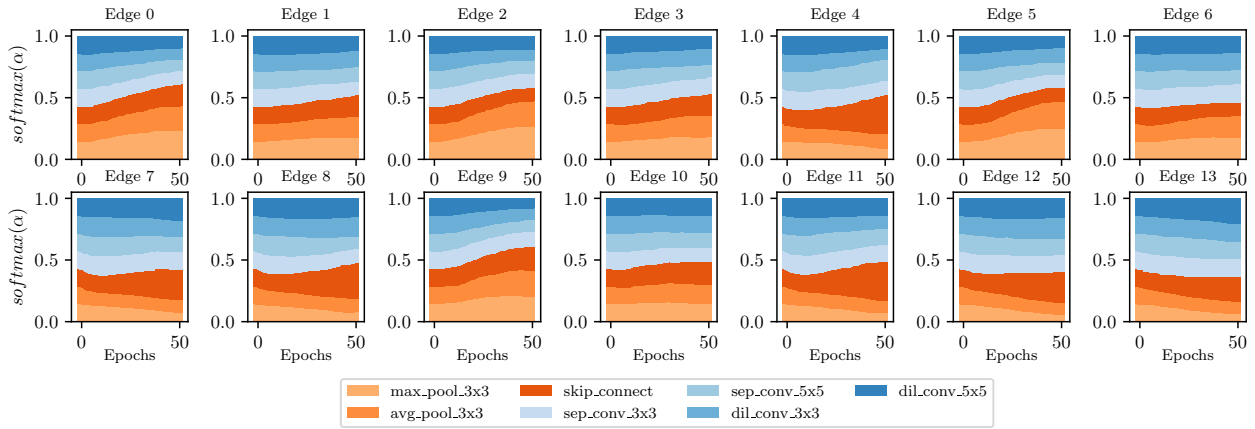


Figure 21. The sigmoid evolution when running Fair DARTS with bi-level optimization in  $S_1$ .

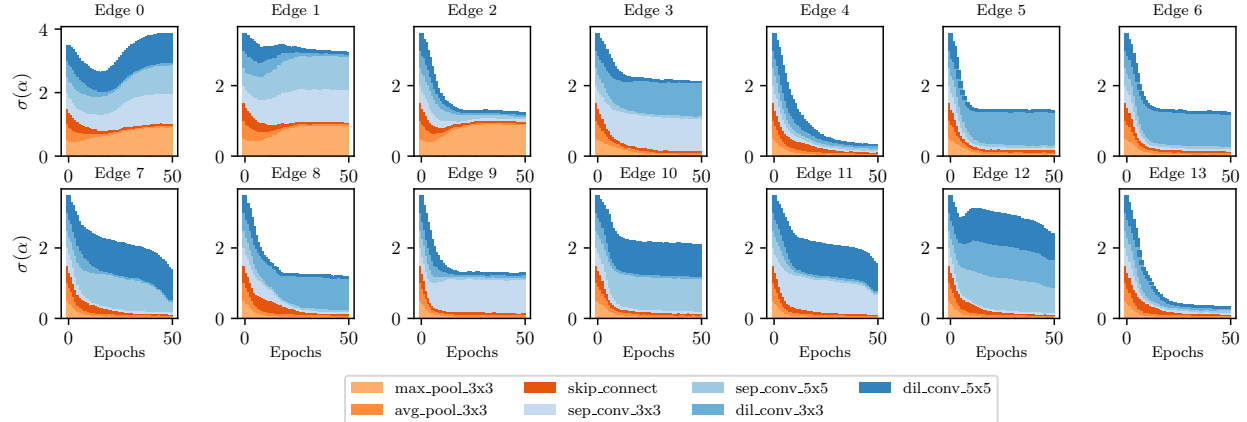


(a) Normal Cell

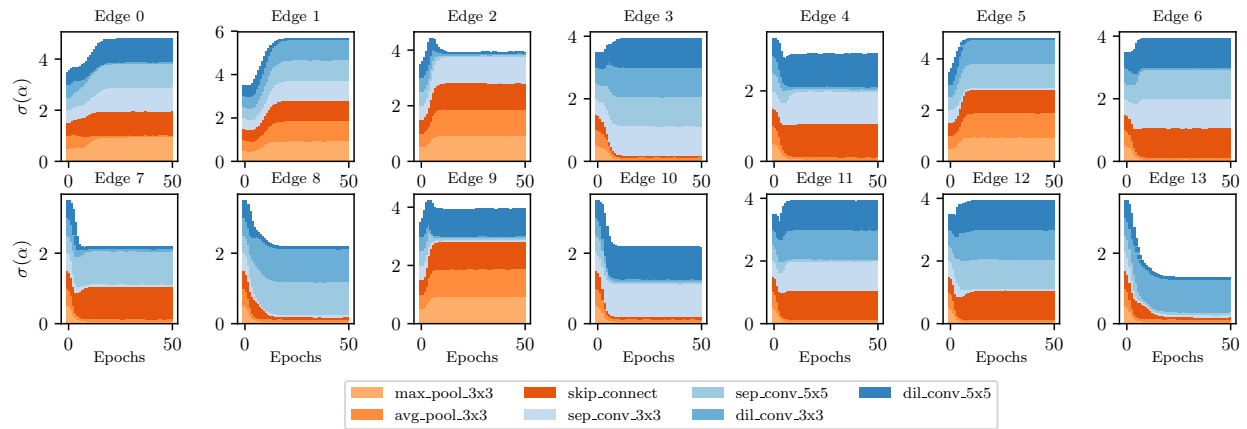


(b) Reduction Cell

Figure 22. The evolution of  $softmax(\alpha)$  when running DARTS on CIFAR-10 in  $S_1$ . Skip connections on edge 0,2,4,5,11 in the normal cell and edge 4,7,8,11,12 in the reduction cell gradually suppress others caused by unfair advantage.

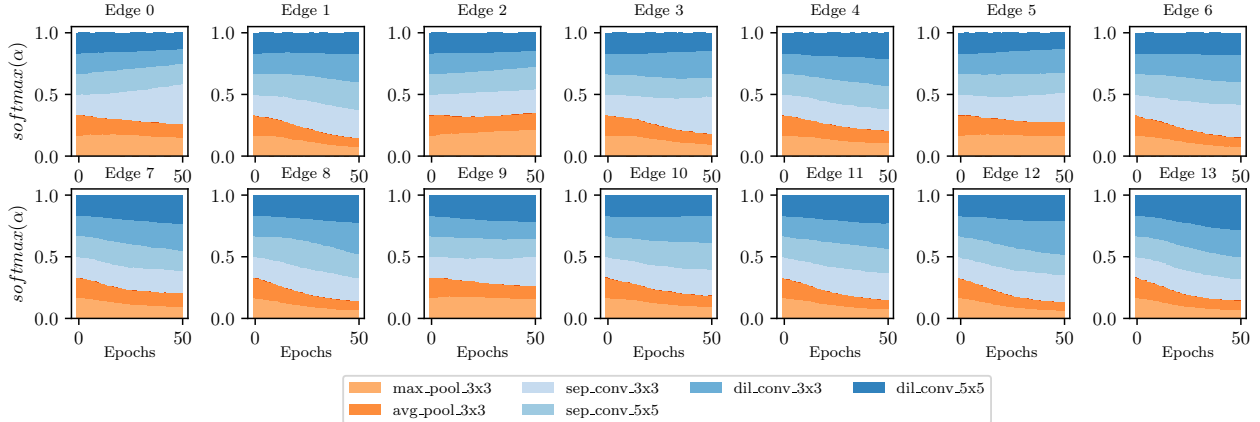


(a) Normal Cell

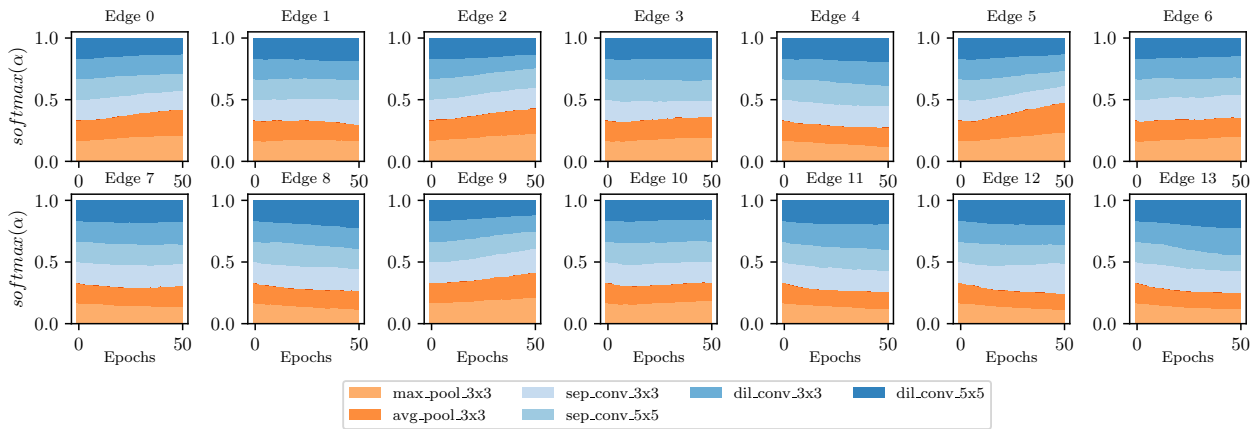


(b) Reduction Cell

Figure 23. The evolution of  $\sigma(\alpha)$  when running Fair DARTS on CIFAR-10 in  $S_1$ . Skip connections enjoy an equal opportunity under collaborative competition. See edge 1,8,12 in normal cell and almost all edges in reduction cell.



(a) Normal Cell



(b) Reduction Cell

Figure 24. The evolution of  $\sigma(\alpha)$  when running DARTS on CIFAR-10 in  $S_1$  without skip connections. With unfair advantages removed, all operations are encouraged to demonstrate each real strength.

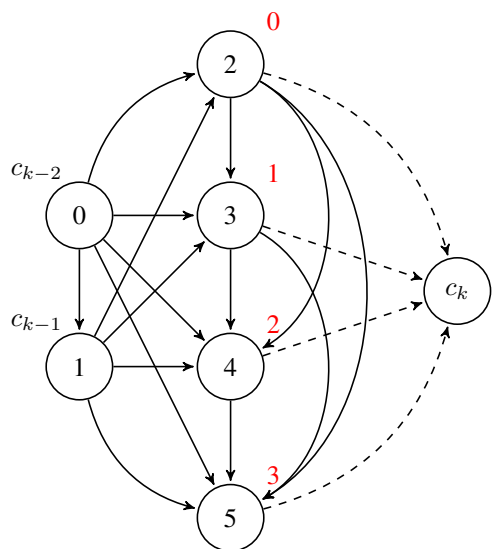


Figure 25. The DARTS search space at cell-level. Red labels indicate intermediate nodes. The outputs of all intermediate nodes are concatenated to form the output  $c_k$ .